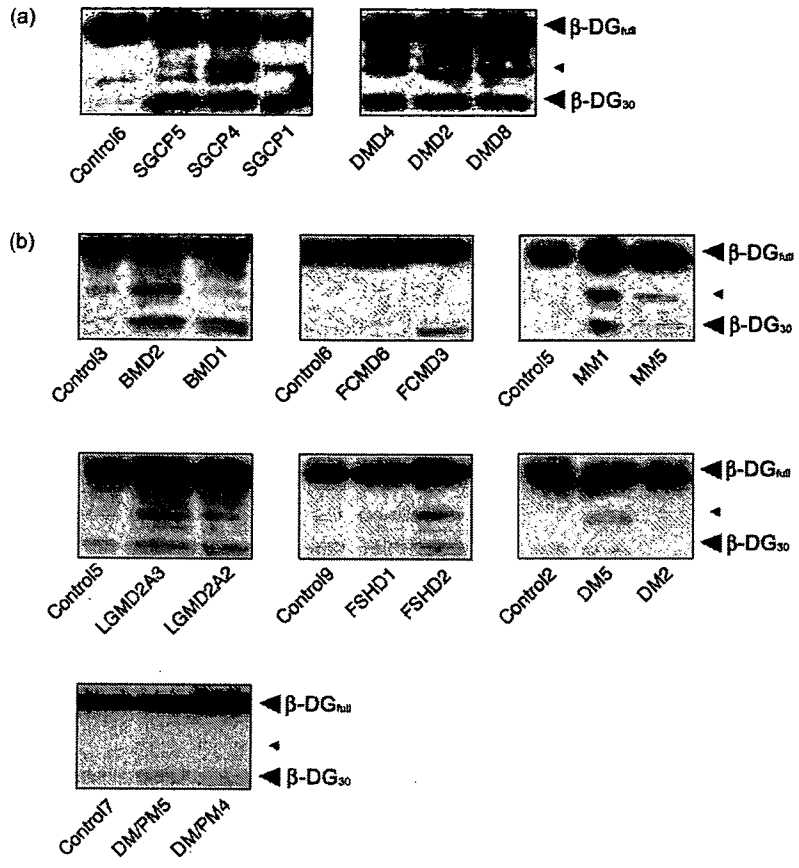

Fig. 2. Immunoblot analysis of β-dystroglycan in the skeletal muscle biopsy specimens of various muscular diseases.The skeletal muscle biopsy specimens were analyzed by immunoblotting using the monoclonal antibody 43DAG/8D5. SGCP and DMD are shown in (a) and BMD, FCMD, MM, LGMD2A, FSHD, DM and DM/PM are shown in (b). Except DMD, equal amount of proteins were loaded for each lane, using myosin heavy chain as internal standard as described previously [10]. For DMD, approximately three times volume of normal control was loaded to visualize β-dystroglycan which is severely reduced in this disease [17]. The band indicated by the small a nrrowhead corresponds to what we reported previously as the intermediate proteolytic fragment of $\beta\text{-DG}_{full}$ [6,7].

was variable not only among the different disease groups but also among the patients with the same disease (Fig. 3). Overall, however, necrotic muscle fibers were observed most frequently in DM/PM, and less frequently in DMD, SGCP and MM (Fig. 3). Hypercontracted muscle fibers were observed most frequently in DMD and SGCP, and less frequently in BMD, DM/PM and FCMD (Fig. 3). Necrotic and hypercontracted muscle fibers were observed infrequently in the other diseases (Fig. 3). Interstitial fibrosis and infiltration of inflammatory cells were mostprominent in FCMD and DM/PM, respectively (Fig. 3).

4. Discussion

Disruption of the tight linkage between the ECM and cell membrane provided by the dystroglycan complex is presumed to have a deleterious effect on the stability of sarcolemma and viability of muscle cells [2,3,6]. Several mechanisms are conceivable that disrupt this linkage. One is the defective glycosylation of β-dystroglycan, which has been demonstrated in several forms of severe congenital muscular dystrophies [for review, see 12–15]. In these diseases, primary defects of the genes encoding the putative glycosyltransferases disturb the glycosylation of β-dystroglycan crucial for the binding of laminin [16] and result in the disruption of the ECM-cell membrane linkage via the dystroglycan complex [12–15]. Recent evidence indicates that the interaction of a glycosyltransferase LARGE with the N-terminal domain of β-dystroglycan is necessary to initiate the posttranslational glycosylation within the mucin domain of β-dystroglycan [17]. The MMP activity that cleaves the extracellular domain of β-dystroglycan is another mechanism that can disrupt this linkage [6]. In the previous study, we showed that this MMP activity was activated in the skeletal and cardiac muscles of cardiomyopathic hamsters, the model animals of SGCP, resulting in the disruption of the dystroglycan complex [7]. Importantly, we showed that this phenomenon was not an in vitro artifact but rather occurred in vivo [7].

In this study, we investigated the proteolysis of β-dystroglycan in the biopsied skeletal muscles of various

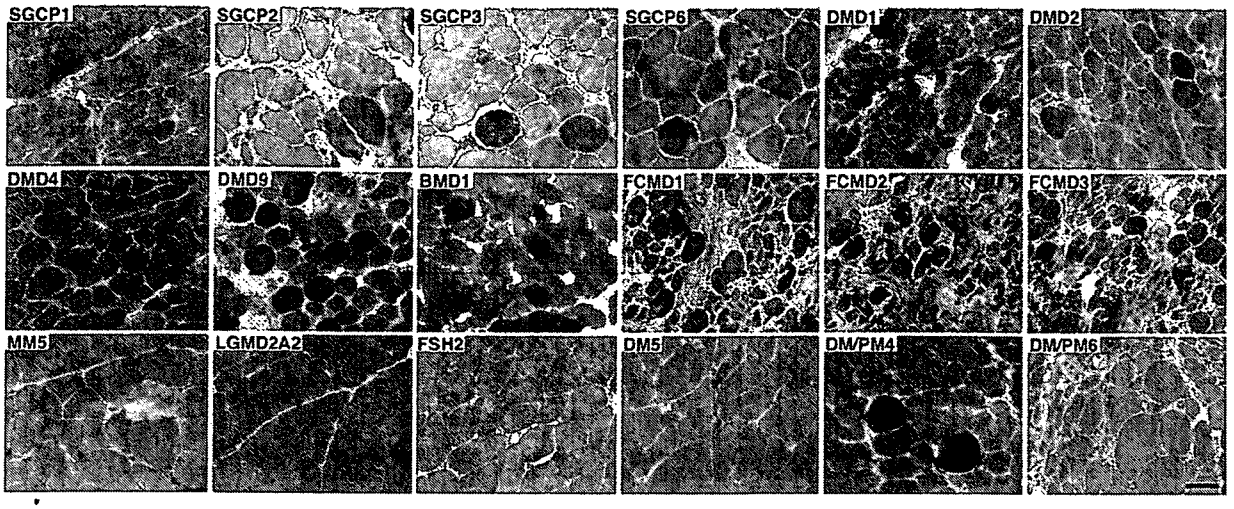

Fig. 3. Histochemical analysis of the skeletal muscle biopsy specimens.The skeletal muscle biopsy specimens were analyzed by staining with hematoxylin and eosin. The severity of the pathological changes was variable not only among the different disease groups but also among the patients with the same disease. Overall, necrotic muscle fibers were observed most frequently in DM/PM, and less frequently in DMD, SGCP and MM. Hypercontracted muscle fibers were observed most frequently in DMD and SGCP, and less frequently in BMD, DM/PM and FCMD. Necrotic and hypercontracted muscle fibers were infrequently observed in the other diseases. Interstitial fibrosis and infiltration of inflammatory cells were most prominent in FCMD and DM/PM, respectively. Bar, 50 μm.

human muscular diseases. We found that the proteolysis of β-dystroglycan was increased significantly in SGCP and DMD. The present results confirm the previous observation by Anderson and Davison, who referred to a similar phenomenon in the biopsied skeletal muscles of SGCP patients [11]. However, they attributed this to the artificial degradation and did not present the results in details [11]. Together with the aforementioned results in cardiomyopathic hamsters [7], we propose that the proteolysis of β-dystroglycan in SGCP is not an in vitro artifact but rather occurs in vivo. On the other hand, this study is the first to report the increased proteolysis of β-dystroglycan in DMD.

At present, the mechanism by which the proteolysis of β-dystroglycan is increased in SGCP and DMD remains obscure. In this respect, it should be noted that hypercontracted muscle fibers were observed frequently in the patients with SGCP and DMD, raising a possibility that the proteolysis of β-dystroglycan may reflect the active degeneration process of muscle fibers. However, the proteolysis of β-dystroglycan was not severe in the patients with BMD and DM/PM who had numerous hypercontracted muscle fibers (for instance, BMD1 and DM/PM4 of Fig. 3). These results suggest that other or additional mechanisms may be present that contribute to the proteolysis of β-dystroglycan. For instance, it is possible that the deficiency of the sarcoglycan complex may render β-dystroglycan susceptible to proteolysis, because it is well established that the sarcoglycan complex is specifically and drastically reduced in these two diseases [18]. In any case, the resulting proteolysis of β-dystroglycan will disrupt the link between the ECM and cell membrane via the dystroglycan complex and render muscle fibers susceptible to further degeneration.

The proteolysis of β-dystroglycan was not significantly increased in BMD, FCMD, MM, LGMD2A, FSHD, DM and DM/PM, although mild proteolysis was detectable in some individuals. When we initiated this study, we were particularly interested if the proteolysis of β-dystroglycan by MMP was activated in FCMD. In FCMD skeletal muscle, the glycosylation of β-dystroglycan crucial for the binding of laminin is disturbed, resulting in the disruption of the ECM-cell membrane linkage via the dystroglycan complex [19]. We wondered if this might render β-dystroglycan susceptible to proteolysis but have found that this is not the case in this study. We also wondered if the proteolysis of β-dystroglycan was increased in DM/PM, because various MMPs are reported activated in inflammatory myopathies [20–22]. However, this did not turn out to be the case in this study. Our results suggest that the MMP that cleaves the extracellular domain of β-dystroglycan may be distinct from those reported activated in inflammatory myopathies.

Acknowledgements

We thank Miki Yamanaka and Yuka Sasayama for their expert technical assistance. This work was supported by [1] Research Grants 14B-4 and 16B-1 for Nervous and Mental Disorders (Ministry of Health, Labor and Welfare), [2] Research on Psychiatric and Neurological Diseases and Mental Health (Ministry of Health, Labor and Welfare), and [3] Research Grant 16390256 and 'High-Tech Research Center' Project for Private Universities: matching fund subsidy from MEXT (Ministry of Education, Culture, Sports, Science and Technology), 2004–2008.

References

[1] Ibraghimov-Beskrovnaya O, Ervasti JM, Leveille CJ, Slaughter CA, Sernett SW, Campbell KP. Primary structure of dystrophin-associated glycoproteins linking dystrophin to the extracellular matrix. Nature 1992;355:696–702.

[2] Henry MD, Campbell KP. Dystroglycan: an extracellular matrix receptor linked to the cytoskeleton. Curr Opin Cell Biol 1996;8:625–31.

[3] Winder SJ. The complexities of dystroglycan. Trends Biochem Sci 2001;26:118–24.

[4] Stasio ED, Sciandra F, Maras B, et al. Structural and functional analysis of the N-terminal extracellular region of β-dystroglycan. Biochem Biophys Res Comm 1999;206:274–8.

[5] Ishikawa-Sakurai M, Yoshida M, Imamura M, Davies KE, Ozawa E. ZZ domain is essentially required for the physiological binding of dystrophin and utrophin to β-dystroglycan. Hum Molec Genet 2004; 13:693–702.

[6] Yamada H, Saito F, Fukuta-Ohi H, et al. Processing of β-dystroglycan by matrix metalloproteinase disrupts the link between the extracellular matrix and cell membrane via the dystroglycan complex. Hum Molec Genet 2001;10:1563–9.

[7] Matsumura K, Arai K, Zhong D, et al. Disruption of dystroglycan axis by β-dystroglycan processing in cardiomyopathic hamster muscle. Neuromusc Disord 2003;13:796–803.

[8] Nigro V, Okazaki Y, Belsito A, et al. Identification of the Syrian hamster cardiomyopathy gene. Hum Molec Genet 1997; 6:601–7.

[9] Sakamoto A, Ono K, Abe M, et al. Both hypertrophic and dilated cardiomyopathies are caused by mutation of the same gene, δ-sarcoglycan, in hamster: an animal model of disrupted dystrophin-associated glycoprotein complex. Proc Natl Acad Sci USA 1997;94: 13873–8.

[10] Matsumura K, Tome FMS, Collin H, et al. Deficiency of the 50K dystrophin-associated glycoprotein in severe childhood autosomal recessive muscular dystrophy. Nature 1992;359:320–2.

[11] Anderson LVB, Davison K. Multiplex western blotting system for the analysis of muscular dystrophy patients. Am J Pathol 1999;154: 1017–22.

[12] Martin-Rendon E, Blake DJ. Protein glycosylation in disease: new insights into the congenital muscular dystrophies. Trends Pharmacol Sci 2003;24:178–83.

[13] Grewal PK, Hewitt JE. Glycosylation defects: a new mechanism for muscular dystrophy? Hum Molec Genet 2003;12: 259–64.

[14] Endo T, Toda T. Glycosylation in congenital muscular dystrophies. Biol Pharm Bull 2003;26:1641–7.

[15] Muntoni F, Brockington M, Torelli S, Brown SC. Defective glycosylation in congenital muscular dystrophies. Curr Opin Neurol 2004;17:205–9.

[16] Chiba A, Matsumura K, Yamada H, et al. Structures of sialylated O-linked oligosaccharides of bovine peripheral nerve α-dystroglycan: the role of a novel mannosyl type oligosaccharide in the binding with laminin. J Biol Chem 1997;272:2156–62.

[17] Kanagawa M, Saito F, Kunz S, et al. Molecular recognition by LARGE is essential for expression of functional dystroglycan. Cell 2004;117:953–64.

[18] Ohlendieck K, Matsumura K, Ionasescu VV, et al. Duchenne muscular dystrophy: deficiency of dystrophin-associated proteins in the sarcolemma. Neurology 1993;43:795–800.

[19] Michele DE, Barresi R, Kanagawa M, et al. Post-translational disruption of dystroglycan–ligand interactions in congenital muscular dystrophies. Nature 2002;418:417–22.

[20] Choi YC, Dalakas MC. Expression of matrix metalloproteinases in the muscle of patients with inflammatory myopathies. Neurology 2000; 54:65–71.

[21] Kieseier BC, Schneider C, Clements JM, et al. Expression of specific matrix metalloproteinases in inflammatory myopathies. Brain 2001; 124:341–51.

[22] Schoser BG, Blottner D, Stuerenburg HJ. Matrix metalloproteinases in inflammatory myopathies: enhanced immunoreactivity near atrophic myofibers. Acta Neurol Scand 2002;105:309–13.

FEBS 29463 FEBS Letters 579 (2005) 2359–2363

Aberrant glycosylation of α-dystroglycan causes defective binding of laminin in the muscle of chicken muscular dystrophy

Fumiaki Saito[a,*], Martina Blank[b], Jörn Schröder[b], Hiroshi Manya[c], Teruo Shimizu[a], Kevin P. Campbell[d], Tamao Endo[c], Makoto Mizutani[e], Stephan Kröger[b], Kiichiro Matsumura[a]

[a] *Department of Neurology and Neuroscience, Teikyo University, 2-11-1 Kaga, Itabashi-ku, Tokyo 173-8605, Japan*
[b] *Institute for Physiological Chemistry, University of Mainz, Duesbergweg 6, D-55099 Mainz, Germany*
[c] *Glycobiology Research Group, Tokyo Metropolitan Institute of Gerontology, 35-2 Sakae-chyo, Itabashi-ku, Tokyo 173-0015, Japan*
[d] *Howard Hughes Medical Institute, Department of Physiology and Biophysics and Department of Neurology, The University of Iowa, Roy J. and Lucille A. Carver College of Medicine, 400 Eckstein medical research building, Iowa City, IA 52242-1101, USA*
[e] *Nippon Institute for Biological Science, 3331-114 kamisasao, kobuchisawa-chyo, Yamanashi prefecture 408-0041, Japan*

Received 17 February 2005; revised 9 March 2005; accepted 9 March 2005

Available online 25 March 2005

Edited by Sandro Sonnino

Abstract Dystroglycan is a central component of dystrophin–glycoprotein complex that links extracellular matrix and cytoskeleton in skeletal muscle. Although dystrophic chicken is well established as an animal model of human muscular dystrophy, the pathomechanism leading to muscular degeneration remains unknown. We show here that glycosylation and laminin-binding activity of α-dystroglycan (α-DG) are defective in dystrophic chicken. Extensive glycan structural analysis reveals that Galβ1-3GalNAc and GalNAc residues are increased while Siaα2-3Gal structure is reduced in α-DG of dystrophic chicken. These results implicate aberrant glycosylation of α-DG in the pathogenesis of muscular degeneration in this model animal of muscular dystrophy.

Keywords: Dystroglycan; Laminin; Muscular dystrophy; Glycosylation; Dystrophic chicken

1. Introduction

The dystroglycan complex is composed of two proteins, α- and β-dystroglycan (α- and β-DG), which are encoded by a single gene and cleaved by posttranslational processing [1]. α-DG is a highly glycosylated extracellular peripheral membrane protein and binds to several extracellular matrix (ECM) proteins including laminin, agrin, and perlecan [2–4]. In turn, the transmembrane protein β-DG anchors α-DG at the extracellular surface of the plasma membrane, while its cytoplasmic domain interacts with dystrophin, a large cytoplasmic protein that binds to F-actin [5]. Thus, the DG complex plays a crucial role to stabilize the plasma membrane by acting as an axis through which the ECM is tightly linked to the cytoskeleton.

Recently, primary mutations in the genes encoding putative glycosyltransferases have been identified in several types of congenital muscular dystrophies including Fukuyama-type congenital muscular dystrophy, muscle–eye–brain disease, Walker–Warburg syndrome, congenital muscular dystrophy 1C (MDC1C) and 1D (MDC1D) [6–10]. Because glycosylation and laminin-binding activity of α-DG are defective in these diseases [11], they are collectively called α-dystroglycanopathy [12]. However, the precise oligosaccharide structures defective in α-dystroglycanopathy have not been elucidated.

Muscular dystrophy in chicken was first described in 1956 [13]. Although dystrophic chicken has been established as an animal model of muscular dystrophy, the primary mutation has not yet been identified [14] and the pathomechanism leading to muscle cell degeneration remains unknown. We demonstrate here that glycosylation and laminin-binding activity of α-DG are defective in the skeletal muscle of dystrophic chicken. Extensive glycan structural analysis reveals that, compared to control chicken, the amount of Galβ1-3GalNAc and GalNAc residues are increased, whereas Siaα2-3Gal structure is reduced in α-DG of dystrophic chicken.

2. Materials and methods

2.1. Antibodies

Mouse monoclonal antibody against sugar chain moiety of α-DG (IIH6) and sheep polyclonal antibody against core protein of α-DG (sheep anti-α-DG) were described previously [2,15]. Mouse monoclonal antibody against sugar chain moiety of α-DG (IVA4-1) was obtained from Upstate Biotechnology. Mouse monoclonal antibody against β-DG (8D5), β-sarcoglycan (5B1) and γ-sarcoglycan (21B5) were kind gifts from Dr. L.V.B. Anderson (Newcastle General Hospital). Mouse monoclonal anti-dystrophin (MANDRA 1) and affinity isolated rabbit anti-laminin were obtained from Sigma. Mouse monoclonal anti-dystrobrevin was purchased from BD Biosciences.

2.2. Lectin chromatography

Dystrophic chicken used in this study is New Hampshire, line 413, the colony of which is maintained homozygously. Line GSN/1, was used as a control. Pectoralis muscle of dystrophic and control chicken of 3 months of age were used. Skeletal muscle was disrupted with a polytron followed by Daunce homogenization and incubation in 50 mM Tris–HCl, pH 7.4, 500 mM NaCl, 1% Triton X-100, 0.6 μg/ml pepstatin A, 0.5 μg/ml leupeptin, 0.5 μg/ml aprotinin, 0.75 mM benzamidine, and 0.1 mM PMSF. The extract was incubated with lectin

*Corresponding author. Fax: +813 3964 6394.
E-mail address: f-saito@med.teikyo-u.ac.jp (F. Saito).

Abbreviations: DG, dystroglycan; DGC, dystrophin–glycoprotein complex

0014-5793/$30.00
doi:10.1016/j.febslet.2005.03.033

agarose, including wheat germ agglutinin (WGA), concanavalin A (Con A), peanut agglutinin (PNA), *Vicia villosa* agglutinin isolectin B_4 (VVA-B_4), *Maackia amurensis* lectin (MAM) and lentil lectin (LCA). Bound proteins were eluted by boiling the beads in sample buffer (65 mM Tris–HCl, pH 6.9, 3% SDS, 1% β-mercaptoethanol, 115 mM sucrose, and 0.0004% bromophenol blue) and the eluates were analyzed by Western blotting using sheep anti-α-DG.

2.3. Miscellaneous

Chemical deglycosylation was described previously [2]. Sialidase digestion was performed using sialidase from *Clostridium perfringens* (Roche) according to the procedure described elsewhere [16]. Immunofluorescent microscopic analysis, Western blotting and blot overlay assay were performed as described elsewhere [11]. The amount of glycosidically bound sialic acid was compared by periodate–resorcinol method [17] and statistical significance was evaluated by *t* test. Solid-phase assay was performed as previously mentioned [11] except that WGA eluates were coated on 96 wells EIA/RIA plates (Coaster) after measuring the band intensity of α-DG on Western blots so that each well contained the same amount of α-DG.

3. Results

3.1. Decreased immunoreactivity of α-DG in the skeletal muscle of dystrophic chicken

We first performed immunofluorescent microscopic analysis. The immunoreactivity of α-DG revealed by antibody against sugar chain moiety of α-DG was significantly decreased in dystrophic chicken, whereas the immunoreactivity of α-DG was indistinguishable between control and dystrophic chicken when detected by antibody against core protein of α-DG. The other components of dystrophin–glycoprotein complex (DGC) were normally expressed in dystrophic chicken (Fig. 1). Consistent with the immunofluorescent analysis, Western blotting with antibody against sugar chain moiety of α-DG demonstrated reduced immunoreactivity of α-DG in dystrophic chicken (Fig. 2). In addition, α-DG of dystrophic chicken migrated at 160 kD, faster than that of control which migrated at 200 kD (Fig. 2). The expression and molecular mass of the other components of the DGC were not altered (Fig. 2).

3.2. Altered glycosylation of α-DG in the skeletal muscle of dystrophic chicken

The results described above raise the possibility that the glycosylation, rather than expression, of α-DG in dystrophic chicken may be altered. In order to test this possibility, α-DG was enriched by WGA chromatography and chemically deglycosylated with trifluoromethanesulfonic acid. Similar to the antibody against sugar chain moiety of α-DG, antibody against core protein of α-DG recognized α-DG species migrating around 200 and 160 kD in control and dystrophic chicken, respectively (Fig. 3, deglycosylation −). In addition, however, the anti-core protein antibody also detected α-DG species with a lower molecular mass of 110 kD in control and 70–120 kD in dystrophic chicken (Fig. 3, deglycosylation −). In this report, we tentatively call the larger and smaller α-DG species as L-α-dystroglycan (L-α-DG) and S-α-dystroglycan (S-α-DG), respectively. Upon chemical deglycosylation, the molecular mass of α-DG was reduced to 55 kD both in control and dystrophic chicken equally, eliminating the difference in molecular mass (Fig. 3, deglycosylation +). These data indicate that α-DG is aberrantly glycosylated in the skeletal muscle of dystrophic chicken. We also examined various tissues of dystrophic chicken to see if defective glycosylation of α-DG was present. Western blot analysis using antibody against core protein of α-DG demonstrated a

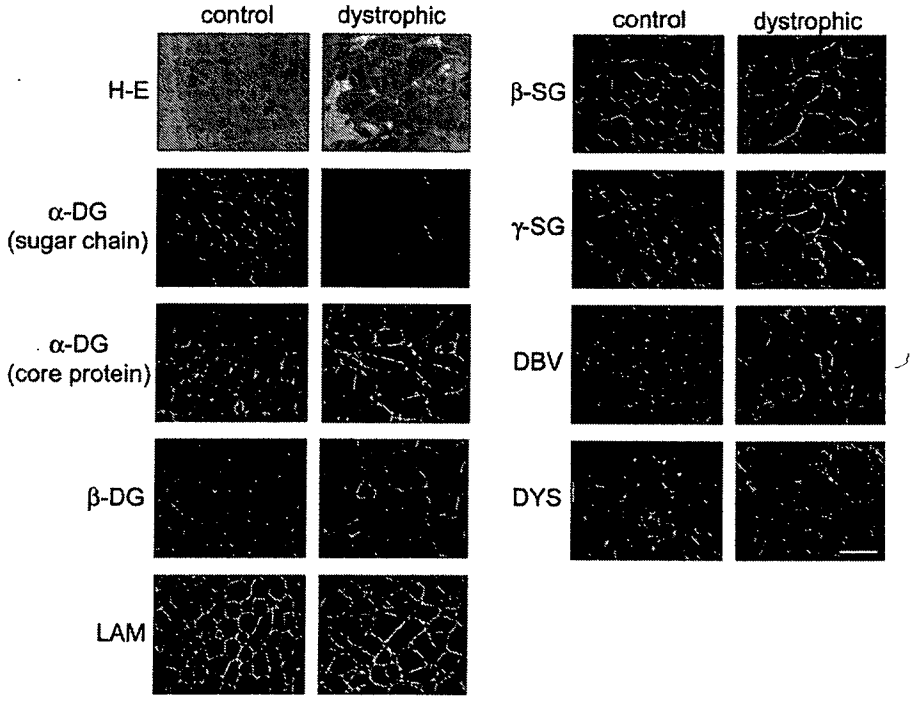

Fig. 1. Immunoreactivity of α-dystroglycan is reduced in the skeletal muscle of dystrophic chicken when probed by antibody against sugar chain moiety. Expression and localization of each component of the DGC were analyzed by immunofluorescent microscopy. The immunoreactivity of α-DG, as revealed by antibody against sugar chain moiety of α-DG (IIH6), is reduced in dystrophic chicken. However, the expression of α-DG core protein is not altered. DG, dystroglycan; LAM, laminin; SG, sarcoglycan; DBV, dystrobrevin; DYS, dystrophin. Bar indicates 100 μm.

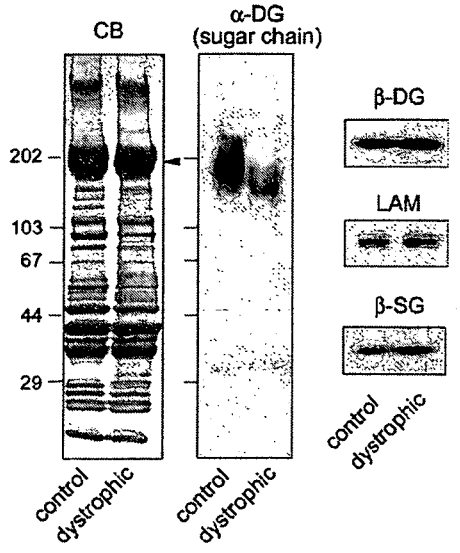

Fig. 2. The molecular mass of α-DG is decreased in the skeletal muscle of dystrophic chicken. Western blotting was performed to examine the expression of α-DG using whole skeletal muscle homogenates. The amount of protein loaded for each lane was normalized using myosin heavy chain as internal standard (arrowhead in the panel CB). α-DG in dystrophic chicken migrates faster than that in control and the immunoreactivity of α-DG is decreased in dystrophic chicken using antibody against sugar chain moiety of α-DG (IIH6). The expression of other components of the DGC is not altered. CB, Coomassie blue staining; DG, dystroglycan; LAM, laminin; SG, sarcoglycan.

downward shift in the molecular mass of α-DG in cardiac muscle, but not in other tissues including brain, peripheral nerve, kidney, spleen and liver (data not shown), indicating

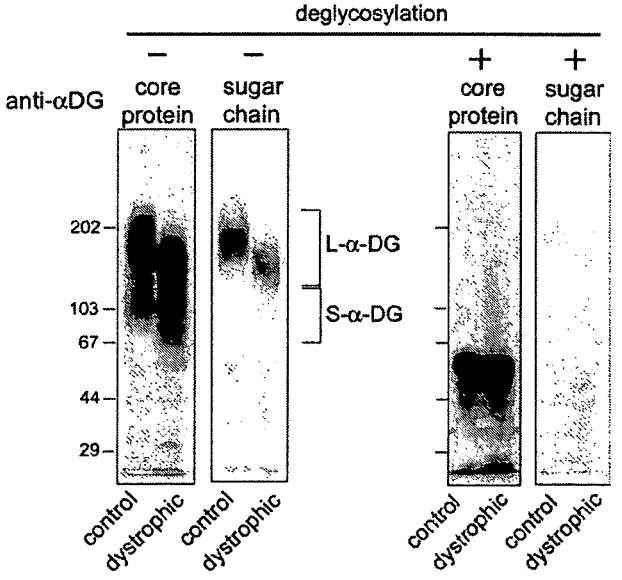

Fig. 3. Deglycosylation eliminates the difference in molecular mass of α-DG between control and dystrophic chicken. α-DG was enriched by WGA chromatography and chemically deglycosylated with trifluoromethanesulfonic acid. Antibody against core protein of α-DG recognizes α-DG species with higher molecular mass (L-α-DG), which are also detected by antibody against sugar chain moiety of α-DG (VIA4-1). In addition, the anti-core protein of α-DG recognizes α-DG species with lower molecular mass (S-α-DG). After deglycosylation, the molecular mass of α-DG decreases to 55 kD in both control and dystrophic chicken equally (deglycosylation +).

that glycosylation of α-DG was also altered in the cardiac muscle of dystrophic chicken.

3.3. Laminin-binding activity of α-DG is decreased in the skeletal muscle of dystrophic chicken

Blot overlay assays demonstrated that the binding of laminin 1 and 2 to α-DG was greatly reduced in dystrophic chicken (Fig. 4A). Notably, both laminin 1 and 2 bound to L-α-DG, but not S-α-DG (Fig. 4A). The band intensity of S-α-DG and L-α-DG was measured and the ratio of S-α-DG against total α-DG (intensity of S-α-DG/intensity of S-α-DG + L-α-DG) was calculated. The ratio of S-α-DG was 16.8 ± 4.5% in control versus 40.9 ± 4.1% in dystrophic chicken (Fig. 4B), indicating that many more α-DG molecules in dystrophic chicken lack the laminin-binding activity than control. Next, we performed quantitative solid-phase assay. The total laminin-binding activity was significantly decreased in the skeletal muscle of dystrophic chicken (Fig. 4C).

3.4. Glycosylation defects of dystrophic chicken α-DG analyzed by lectin chromatography

To investigate the change in glycan structure of α-DG in dystrophic chicken, we performed a set of lectin chromatographies.

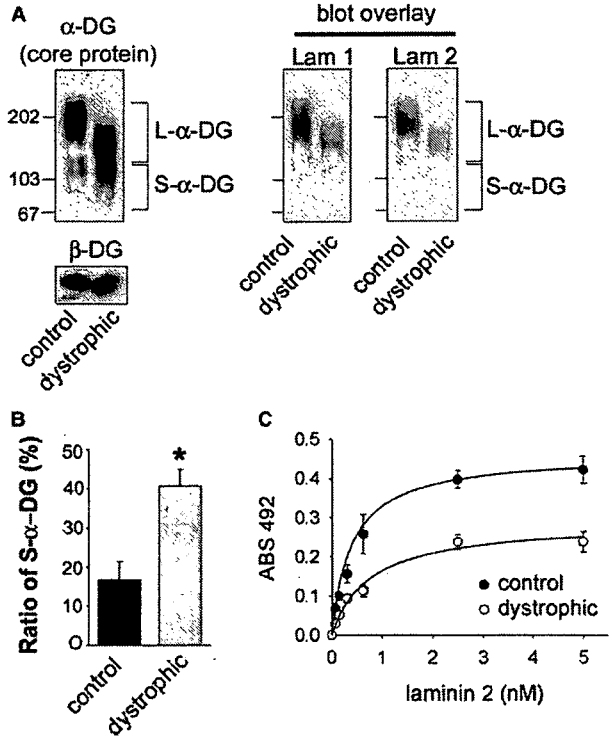

Fig. 4. Laminin-binding activity of α-DG is decreased in the skeletal muscle of dystrophic chicken. (A) Equal amount of DG was transferred to PVDF membranes as revealed by Western blotting for α-DG and β-DG. Blot overlay assays demonstrate that the binding of both laminin 1 and 2 to α-DG is substantially decreased in dystrophic chicken. Both laminin 1 and 2 bind to L-α-DG, but not S-α-DG. Lam 1, laminin 1; Lam 2, laminin 2. (B) The band intensity of L-α-DG and S-α-DG was measured and the ratio of S-α-DG against total α-DG was calculated. The ratio of S-α-DG is significantly higher in dystrophic chicken. $^*P < 0.003$. (C) Solid-phase assay reveals that laminin-binding activity is significantly reduced in the skeletal muscle of dystrophic chicken.

As shown in Fig. 5A, Con A bound most of the α-DG species, whereas LCA had no significant interaction with any α-DG species (Fig. 5A). In sharp contrast, MAM bound L-α-DG in control, while it interacted only weakly with α-DG in dystrophic chicken (Fig. 5A), indicating that Siaα2-3Gal moieties are profoundly reduced in α-DG of dystrophic chicken. Interestingly, PNA bound to a fraction of S-α-DG in dystrophic chicken, while no binding to α-DG occurred in control (Fig. 5B, sialidase −). VVA-B_4 bound weakly to S-α-DG in control, whereas it strongly interacted with L-α-DG and S-α-DG in dystrophic chicken. Because the reactivity of these lectins are known to be severely decreased when sialic acids are attached to non-reducing termini of their binding sugar chain moieties [18], we enzymatically removed sialic acids by sialidase and repeated the experiments. After sialidase digestion, both S-α-DG and L-α-DG extensively interacted with PNA in dystrophic chicken, whereas only a small amount of S-α-DG was recovered in control. These results indicate that Galβ1-3GalNAc moieties are much more abundant on α-DG in dystrophic chicken than that in control (Fig. 5B, sialidase +). Similar result was obtained with VVA-B_4, indicating that GalNAc structures are much more abundant on α-DG of dystrophic chicken (Fig. 5B, sialidase +). The amount of glycosidically bound sialic acids quantified by periodate–resorcinol method was substantially reduced in dystrophic chicken (Fig. 5C), which is consistent with the result of MAM lectin chromatography.

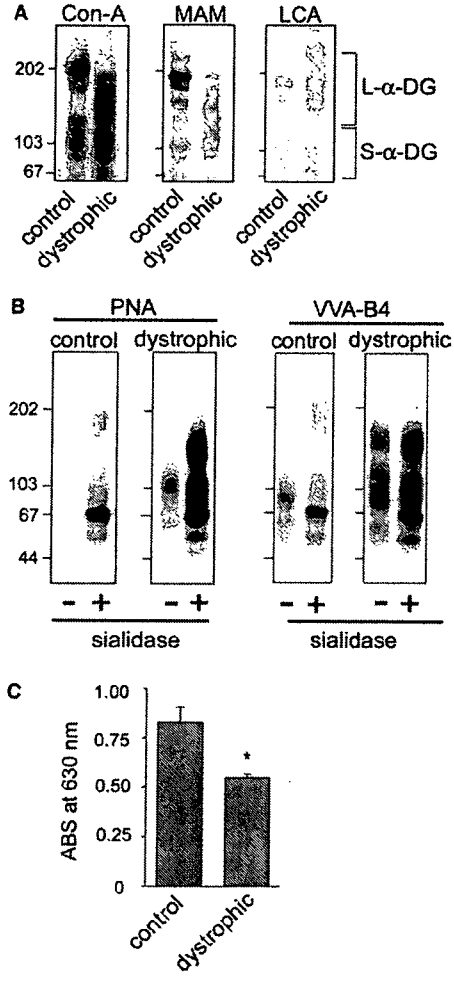

Fig. 5. Glycosylation of α-DG is altered in the skeletal muscle of dystrophic chicken. (A) α-DG was extracted using Triton X-100 and applied to lectin chromatography. The bound α-DG was visualized by Western blotting using antibody against core protein of α-DG. Con-A binds most of the α-DG species, while LCA does not interact with any α-DG species significantly. MAM strongly binds only to L-α-DG in control. (B) The Triton X-100 extracts were applied to PNA or VVA-B_4 chromatography with or without prior digestion by sialidase. Without sialidase treatment, PNA binds S-α-DG in dystrophic chicken, while it does not interact with α-DG in control (sialidase −). VVA-B_4 binds S-α-DG in control only weakly, while it interacts strongly with both L- and S-α-DG in dystrophic chicken (sialidase −). With sialidase digestion, both PNA and VVA-B_4 bind extensively to L-α-DG and S-α-DG in dystrophic chicken compared to control (sialidase +). (C) Quantification of sialic acid by periodate–resorcinol method reveals that the amount of glycosidically bound sialic acids in the skeletal muscle of dystrophic chicken is significantly less than that of control chicken. $^*P < 0.001$.

4. Discussion

The mucin-like domain of α-DG is heavily glycosylated by *O*-linked glycans [19], with the sugar chain moieties constituting up to two-thirds of its total molecular mass [1,2]. The antibody against sugar chain moiety of α-DG detected only L-α-DG, while anti-α-DG core protein detected both L-α-DG and S-α-DG (Figs. 2 and 3), indicating diverse glycosylation of α-DG in vivo. Notably, laminin bound to L-α-DG, but not to S-α-DG, in both control and dystrophic chicken (Fig. 4), indicating that the interaction of laminin with α-DG is strictly regulated through glycosylation of α-DG and that a fraction of α-DG does not possess the sugar chain moieties necessary for the binding of laminin in vivo. Furthermore, the ratio of non-laminin-binding α-DG (S-α-DG) is greatly increased in dystrophic chicken compared to control (Fig. 4). It would be intriguing to postulate that the increase of non-laminin-binding α-DG may contribute to the dystrophic phenotype by exerting a dominant negative effect in dystrophic chicken, where non-laminin-binding α-DG competes with laminin-binding α-DG for the cytoskeletal linkage via dystrophin. Consistent with this hypothesis, we have observed that adenovirus mediated gene transfer of non-laminin-binding α-DG constructs results in the degeneration of skeletal muscle in mice (Saito and Campbell, unpublished observation).

The results of lectin chromatography indicate that, compared to control chicken, the amount of Galβ1-3GalNAc and GalNAc residues are increased significantly while Siaα2-3Gal structure is severely decreased in α-DG of dystrophic chicken (Fig. 5). The reduction in the amount of sialic acids was confirmed by periodate–resorcinol sialic acid assay (Fig. 5). However, α-DG appears to be hyposialylated rather than asialylated (Fig. 5C). We have reported recently that hyposialylation of α-DG alone is not enough to abolish its laminin-binding activity in vivo [20]. It remains to be determined if hyposialylation in dystrophic chicken reflects the reduction of the sialyl *O*-mannosyl glycan, Sia2-3Galβ1-4GlcNAcβ1-2Man-Ser/Thr, implicated in the binding of laminin [21,22].

Pavoni et al. [23] reported recently that antibody against C-terminal portion of α-DG core protein detected α-DG with molecular mass of 109 kD in the skeletal muscle of normal chicken. Our S-α-DG may correspond to this small α-DG, as judged by molecular mass. Pavoni et al. further postulated that this 109 kD α-DG might be a partially glycosylated form of

α-DG. In the present study, we provided clear evidence of actual alteration of glycosylation of this small α-DG molecule (Figs. 3 and 5). The molecular mass of α-DG in the skeletal muscle of normal chicken was reported to change during development [24]. It would be thus interesting to see if the molecular mass of α-DG in the skeletal muscle of dystrophic chicken also changes during development by future studies.

In conclusion, we have demonstrated altered glycosylation and decreased laminin-binding activity of α-DG in chicken muscular dystrophy. Furthermore, we have demonstrated that Siaα2-3Gal structure is reduced, while Galβ1-3GalNAc and GalNAc moieties are increased on α-DG of this animal model of muscular dystrophy. These data would contribute to further understand the molecular mechanism of muscular degeneration caused by disturbed glycosylation of α-DG in human muscular dystrophies.

Acknowledgments: We thank Hiroko F. Ohi, Miki Yamanaka and Yuka Sasayama for their expert technical assistance. This work was supported by [1] Research Grants 14B-4 and 16B-1 for Nervous and Mental Disorders (Ministry of Health, Labor and Welfare), [2] Research on Psychiatric and Neurological Diseases and Mental Health (Ministry of Health, Labor and Welfare), [3] Research Grant 16390256 and "High-Tech Research Center" Project for Private Universities: matching fund subsidy from MEXT (Ministry of Education, Culture, Sports, Science and Technology), 2004–2008, and [4] a research grant from the Ichiro Kanahara Foundation.

References

[1] Ibraghimov-Beskrovnaya, O., Ervasti, J.M., Leveille, C.J., Slaughter, C.A., Sernett, S.W. and Campbell, K.P. (1992) Primary structure of dystrophin-associated glycoproteins linking dystrophin to the extracellular matrix. Nature 355, 696–702.

[2] Ervasti, J.M. and Campbell, K.P. (1993) A role for the dystrophin–glycoprotein complex as a transmembrane linker between laminin and actin. J. Cell. Biol. 122, 809–823.

[3] Bowe, M.A., Deyst, K.A., Leszyk, J.D. and Fallon, J.R. (1994) Identification and purification of an agrin receptor from Torpedo postsynaptic membranes: a heteromeric complex related to the dystroglycans. Neuron 12, 1173–1180.

[4] Peng, H.B., Ali, A.A., Daggett, D.F., Rauvala, H., Hassell, J.R. and Smalheiser, N.R. (1998) The relationship between perlecan and dystroglycan and its implication in the formation of the neuromuscular junction. Cell Adhes. Commun. 5, 475–489.

[5] Jung, D., Yang, B., Meyer, J., Chamberlain, J.S. and Campbell, K.P. (1995) Identification and characterization of the dystrophin anchoring site on β-dystroglycan. J. Biol. Chem. 270, 27305–27310.

[6] Kobayashi, K., Nakahori, Y., Miyake, M., Matsumura, K., Kondo-Iida, E., Nomura, Y., Segawa, M., Yoshioka, M., Saito, K., Osawa, M., Hamano, K., Sakakihara, Y., Nonaka, I., Nakagome, Y., Kanazawa, I., Nakamura, Y., Tokunaga, K. and Toda, T. (1998) An ancient retrotransposal insertion causes Fukuyama-type congenital muscular dystrophy. Nature 394, 388–392.

[7] Yoshida, A., Kobayashi, K., Manya, H., Taniguchi, K., Kano, H., Mizuno, M., Inazu, T., Mitsuhashi, H., Takahashi, S., Takeuchi, M., Herrmann, R., Straub, V., Talim, B., Voit, T., Topaloglu, H., Toda, T. and Endo, T. (2001) Muscular dystrophy and neuronal migration disorder caused by mutations in a glycosyltransferase, POMGnT1. Dev. Cell 1, 717–724.

[8] Beltran-Valero De Bernabe, D., Currier, S., Steinbrecher, A., Celli, J., Van Beusekom, E., Van Der Zwaag, B., Kayserili, H., Merlini, L., Chitayat, D., Dobyns, W.B., Cormand, B., Lehesjoki, A.E., Cruces, J., Voit, T., Walsh, C.A., van Bokhoven, H. and Brunner, H.G. (2002) Mutations in the *O*-mannosyltransferase gene POMT1 give rise to the severe neuronal migration disorder Walker–Warburg syndrome. Am. J. Hum. Genet. 71, 1033–1043.

[9] Brockington, M., Blake, D.J., Prandini, P., Brown, S.C., Torelli, S., Benson, M.A., Ponting, C.P., Estournet, B., Romero, N.B., Mercuri, E., Voit, T., Sewry, C.A., Guicheney, P. and Muntoni, F. (2001) Mutations in the fukutin-related protein gene (FKRP) cause a form of congenital muscular dystrophy with secondary laminin α2 deficiency and abnormal glycosylation of α-dystroglycan. Am. J. Hum. Genet. 69, 1198–1209.

[10] Longman, C., Brockington, M., Torelli, S., Jimenez-Mallebrera, C., Kennedy, C., Khalil, N., Feng, L., Saran, R.K., Voit, T., Merlini, L., Sewry, C.A., Brown, S.C. and Muntoni, F. (2003) Mutations in the human LARGE gene cause MDC1D, a novel form of congenital muscular dystrophy with severe mental retardation and abnormal glycosylation of α-dystroglycan. Hum. Mol. Genet. 12, 2853–2861.

[11] Michele, D.E., Barresi, R., Kanagawa, M., Saito, F., Cohn, R.D., Satz, J.S., Dollar, J., Nishino, I., Kelley, R.I., Somer, H., Straub, V., Mathews, K.D., Moore, S.A. and Campbell, K.P. (2002) Posttranslational disruption of dystroglycan–ligand interactions in congenital muscular dystrophies. Nature 418, 417–422.

[12] Michele, D.E. and Campbell, K.P. (2003) Dystrophin–glycoprotein complex: post-translational processing and dystroglycan function. J. Biol. Chem. 278, 15457–15460.

[13] Asmundson, V.S. and Julian, L.M. (1956) Inherited muscle abnormalityin the domestic fowl. J. Hered. 47, 248–252.

[14] Lee, E.J., Yoshizawa, K., Mannen, H., Kikuchi, H., Kikuchi, T., Mizutani, M. and Tsuji, S. (2002) Localization of the muscular dystrophy AM locus using a chicken linkage map constructed with the Kobe University resource family. Anim. Genet. 33, 42–48.

[15] Herrmann, R., Straub, V., Blank, M., Kutzick, C., Franke, N., Jacob, E.N., Lenard, H.G., Kroger, S. and Voit, T. (2000) Dissociation of the dystroglycan complex in caveolin-3-deficient limb girdlemuscular dystrophy. Hum. Mol. Genet. 9, 2335–2340.

[16] Yamada, H., Chiba, A., Endo, T., Kobata, A., Anderson, L.V., Hori, H., Fukuta-Ohi, H., Kanazawa, I., Campbell, K.P., Shimizu, T. and Matsumura, K. (1996) Characterization of dystroglycan–laminin interaction in peripheral nerve. J. Neurochem. 66, 1518–1524.

[17] Jourdian, G.W., Dean, L. and Roseman, S. (1971) The sialic acids. XI. A periodate–resorcinol method for the quantitative estimation of free sialic acids and their glycosides. J. Biol. Chem. 246, 430–435.

[18] Ervasti, J.M., Burwell, A.L. and Geissler, A.L. (1997) Tissue-specific heterogeneity in α-dystroglycan sialoglycosylation. Skeletal muscle α-dystroglycan is a latent receptor for *Vicia villosa* agglutinin B4 masked by sialic acid modification. J. Biol. Chem. 272, 22315–22321.

[19] Brancaccio, A., Schulthess, T., Gesemann, M. and Engel, J. (1995) Electron microscopic evidence for a mucin-like region in chick muscle α-dystroglycan. FEBS Lett. 368, 139–142.

[20] Saito, F., Tomimitsu, H., Arai, K., Nakai, S., Kanda, T., Shimizu, T., Mizusawa, H. and Matsumura, K. (2004) A Japanese patient with distal myopathy with rimmed vacuoles: Missense mutations in the epimerase domain of the UDP-*N*-acetylglucosamine 2-epimerase/*N*-acetylmannosamine kinase (GNE) gene accompanied by hyposialylation of skeletal muscle glycoproteins. Neuromuscul. Disord. 14, 158–161.

[21] Chiba, A., Matsumura, K., Yamada, H., Inazu, T., Shimizu, T., Kusunoki, S., Kanazawa, I., Kobata, A. and Endo, T. (1997) Structures of sialylated *O*-linked oligosaccharides of bovine peripheral nerve α-dystroglycan. J. Biol. Chem. 272, 2156–2162.

[22] Sasaki, T., Yamada, H., Matsumura, K., Shimizu, T., Kobata, A. and Endo, T. (1998) Detection of *O*-mannosyl glycans in rabbit skeletal muscle α-dystroglycan. Biochim. Biophys. Acta 1425, 599–606.

[23] Pavoni, E., Sciandra, F., Barca, S., Giardina, B., Petrucci, T.C. and Brancaccio, A. (2005) Immunodetection of partially glycosylated isoforms of α-dystroglycan by a new monoclonal antibody against its β-dystroglycan-binding epitope. FEBS Lett. 579, 493–499.

[24] Leschziner, A., Moukhles, H., Lindenbaum, M., Gee, S.H., Butterworth, J., Campbell, K.P. and Carbonetto, S. (2000) Neural regulation of α-dystroglycan biosynthesis and glycosylation in skeletal muscle. J. Neurochem. 74, 70–80.

Available online at www.sciencedirect.com
ScienceDirect
Analytical Biochemistry 357 (2006) 308–310
ANALYTICAL BIOCHEMISTRY
www.elsevier.com/locate/yabio

Notes & Tips

A simple, one-step cloning method to obtain long artificial triplet repeats

Noboru Sasagawa *, Shoichi Ishiura

Department of Life Sciences, Graduate School of Arts and Sciences, University of Tokyo, Tokyo 153-8902, Japan

Received 25 May 2006
Available online 27 June 2006

Tandem trinucleotide repeats are common in the genomes of many organisms. In humans, triplet repeat expansion causes various hereditary diseases such as Huntington's disease [1] and myotonic dystrophy [2–4]. Because these repeats must involve abnormal physiological functions at the transcribed mRNA or translated protein level, it is critical to establish an easy method for making constructs with artificially expanded triplet repeats.

Previously, we reported a method of obtaining long CTG/CAG triplet repeats using a polymerase chain reaction (PCR)[1] with $(CTG)_7$ and $(CAG)_7$ primers without a template (i.e., nontemplate PCR method) [5]. In this method, we needed to ligate the expanded triplet repeat into blunt-ended plasmid vectors. Therefore, we sometimes had difficulty in adapting the codon frame, and if we wanted to use restriction endonucleases with sticky ends, we needed to clone the repeat into a specific cloning vector, such as pUC118, in the first step and then use multiple subcloning steps to obtain the final construction.

Here we report an improved technique for subcloning expanded triplet repeats into vectors with any restriction sites directly (Fig. 1). The primers (10 μM) *Eco*RI–CTG7 (5′-GGAATTCTAACTGCTGCTGCTGCTGCTG-3′) and CAG10 (5′-CAGCAGCAGCAGCAGCAGCAGCA GCAGCAG-3′) were mixed and used for PCR without any template (tube A). We used LA–*Taq* DNA polymerase with GC buffer (TaKaRa, Tokyo, Japan) and a standard PCR protocol consisting of 25 cycles at 95 °C for 15 s, 57 °C for 1 min, and 72 °C for 1.5 min in an Eppendorf Mastercycler personal thermal cycler (Eppendorf Scientific, Hamburg, Germany). The reaction volume was 20 μl. Similarly, 10 μM each of primers *Xba*I–CAG7 (5′-GCTCTAGACAGCAG CAGCAGCAGCAGCAG-3′) and CTG10 (5′-CTGCTG CTGCTGCTGCTGCTGCTGCTG-3′) were mixed, and we conducted another PCR (tube B) in exactly the same way as with tube A. Then we mixed 10 μl each of the solutions from tubes A and B (tube C, final 20 μl) and continued the PCR. The PCR reagents, reaction conditions, and cycle program for tube C were exactly the same as for tubes A and B. The final PCR product was electrophoresed in 1% agarose gels, and the DNA extracted from the agarose was cut using an *Eco*RI/*Xba*I double digestion.

A derivative of the vector pUC118 was used in the experiment and was cut using *Eco*RI and *Nhe*I (note that the *Nhe*I and *Xba*I sites have compatible cohesive ends). The vector and triplet repeat were ligated and then transformed into *Escherichia coli* XL-1 blue. The positive colonies were selected, and the sequence was confirmed using a Beckman CEQ8000 DNA sequencer (Beckman Coulter, Fullerton, CA, USA).

The PCR products from tubes A and B produced a smear (Fig. 2A), indicating that various lengths of tandem repeats with a restriction site at one end were made successfully in tubes A and B. The PCR product from tube C also produced a smear, and we expected it to consist of tandem repeats with restriction sites at both ends (5′ and 3′). We collected the tandem repeats from tube C, cut them using *Eco*RI/*Xba*I, and ligated them into a vector. Fig. 2B shows the result of a tandem repeat successfully ligated into a vector at the predicted restriction site. Sequence analysis revealed that the vector contained a maximum of more than 100 tandem repeats (Fig. 2B, lane 3). This method is suitable for any plasmid vector. We also tested the vector pGEX and had success (data not shown). The upper limit of the number of repeats is dependent on the insert retention capacity of the vector; we always observed instability with more than 100 CTG triplet repeats in a plasmid. It is necessary to determine a suitable vector, including an artificial chromosome, to clone more than 1000 tandem triplet repeats. Nevertheless, the protocol presented here is still effective for cloning long triplet repeats.

* Corresponding author.
E-mail address: csasa@mail.ecc.u-tokyo.ac.jp (N. Sasagawa).

[1] *Abbreviation used:* PCR, polymerase chain reaction.

doi:10.1016/j.ab.2006.06.010

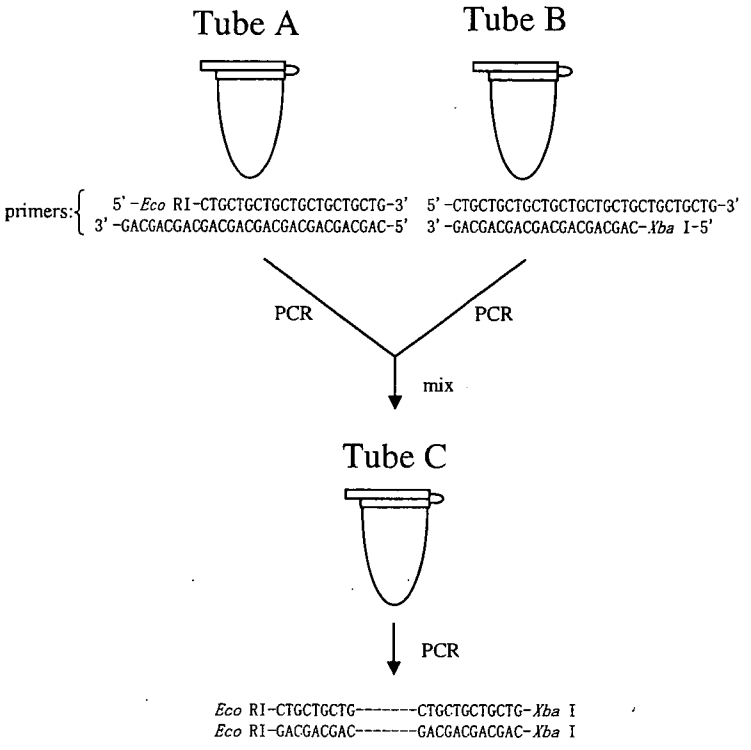

Fig. 1. Scheme used to obtain long triplet repeats with one-step cloning. The final PCR product in tube C consists of various lengths of CTG/CAG repeats with *Eco*RI/*Xba*I sites at each end.

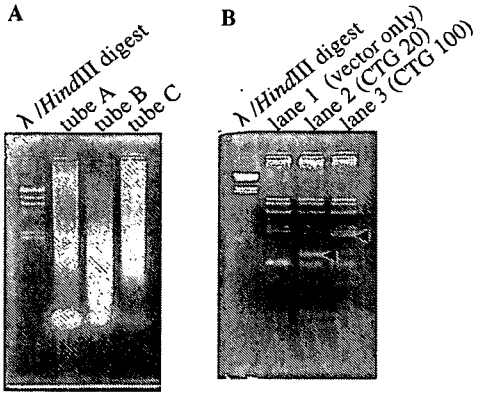

Fig. 2. (A) PCR products from tubes A, B, and C were electrophoresed in 1% agarose gels. All of the lanes show smears, indicating wide variation in the numbers of tandem triplet repeats. (B) The subcloned constructs with the CTG/CAG triplet repeat were cut using *Dra*I and electrophoresed in 2% agarose gels. The arrows show fragments containing the CTG/CAG repeat region. The rate of movement of each band revealed that the clone in lane 3 contains approximately 100 CTG/CAG repeats.

We consider that the key point in this protocol is the use of a proofreading PCR polymerase. Tandem repeats anneal with each other at slipped CTG–CAG repeat positions, and the exonuclease activity of a proofreading polymerase digests the mismatched 3′ end. Then the proofreading polymerase starts a 5′–3′ extension reaction. The repeated reaction of slipped annealing and proofreading extension results in the production of a long tandem repeat. Although we have not tested it, we should be able to skip the tube B step by adding primer *Xba*I–CAG7 to the PCR product in tube A and performing the PCR step in tube C to amplify the desired PCR product.

Consequently, we can make tandem repeat constructs at any desired restriction site. The merit of this method is that we can adopt many other tandem repeats for construction involving one-step ligation.

References

[1] M.E. MacDonald, C.M. Ambrose, M.P. Duyao, R.H. Myers, C. Lin, L. Srinidhi, G. Barnes, S.A. Taylor, M. James, N. Groot, H. MacFarlane, B. Jenkins, M.A. Anderson, N.S. Wexler, J.F. Gusella, G.P. Bates, S. Baxendale, H. Hummerich, S. Kirby, M. North, S. Youngman, R. Mott, G. Zehetner, Z. Sedlacek, A. Poustka, A.-M. Frischauf, H. Lehrach, A.J. Buckler, D. Church, L. Doucette-Stamm, M.C. O'Donovan, L. Riba-Ramirez, M. Shah, V.P. Stanton, S.A. Strobel, K.M. Draths, J.L. Wales, P. Dervan, D.E. Housman, M. Altherr, R. Shiang, L. Thompson, T. Fielder, J.J. Wasmuth, D. Tagle, J. Valdes, L. Elmer, M. Allard, L. Castilla, M. Swaroop, K. Blanchard, F.S. Collins, R. Snell, T. Holloway, K. Gillespie, N. Datson, D. Shaw, P.S. Harper, A novel gene containing a trinucleotide repeat that is expanded and unstable on Huntington's disease chromosomes, Cell 72 (1993) 971–983.

[2] J.D. Brook, M.E. McCurrach, H.G. Harley, A.J. Buckler, D. Church, H. Aburatani, K. Hunter, V.P. Stanton, J.P. Thirion, T. Hudson, R. Sohn, B. Zemelman, R.G. Snell, S.A. Rundle, S. Crow, J. Davies, P. Shelbourne, J. Buxton, C. Jones, V. Juvonen, K. Johnson, P.S. Harper, D.J. Shaw, D.E. Housman, Molecular basis of myotonic dystrophy: expansion of a trinucleotide (CTG) repeat at the 3′ end of a transcript encoding a protein kinase family member, Cell 68 (1992) 799–808.

[3] M. Mahadevan, C. Tsilfidis, L. Sabourin, G. Shutler, C. Amemiya, G. Jansen, C. Neville, M. Narang, J. Barcelo, K. O'Hoy, S. Leblond, J.

Earle-Macdonald, P.J. de Jong, B. Wieringa, R.G. Korneluk, Myotonic dystrophy mutation: an unstable CTG repeat in the 3′ untranslated region of the gene, Science 255 (1992) 1253–1255.

[4] Y.H. Fu, A. Pizzuti, R.G. Fenwick, J. King, S. Rajnarayan, P.W. Dunne, J. Dubel, G.A. Nasser, T. Ashizawa, P.J. de Jong, B. Wieringa, R. Korneluk, M.B. Perryman, H.F. Epstein, C.T. Caskey, An unstable triplet repeat in a gene related to myotonic muscular dystrophy, Science 255 (1992) 1256–1258.

[5] N. Takahashi, N. Sasagawa, K. Suzuki, S. Ishiura, Synthesis of long trinucleotide repeats in vitro, Neurosci. Lett. 262 (1999) 45–48.

PERGAMON

Neuromuscular Disorders 16 (2006) 256–261

www.elsevier.com/locate/nmd

Rapid and accurate diagnosis of facioscapulohumeral muscular dystrophy

Kanako Goto, Ichizo Nishino, Yukiko K. Hayashi *

Department of Neuromuscular Research, National Institute of Neuroscience, National Center of Neurology and Psychiatry (NCNP), 4-1-1 Ogawa-Higashi, Kodaira, Tokyo 187-8502, Japan

Received 10 September 2005; received in revised form 9 January 2006; accepted 18 January 2006

Abstract

Facioscapulohumeral muscular dystrophy (FSHD) is a common muscular disorder, but clinical and genetic complications make its diagnosis difficult. Southern blot analysis detects a smaller sized *Eco*RI fragment on chromosome 4q35 in most facioscapulohumeral muscular dystrophy patients, that contains integral number of 3.3-kb tandem repeats known as D4Z4. The problems for the genetic diagnosis are that southern blotting for facioscapulohumeral muscular dystrophy is quite laborious and time-consuming, and the D4Z4 number is only estimated from the size of the fragment. We developed a more simplified diagnostic method using a long polymerase chain reaction (PCR) amplification technique. Successful amplification was achieved in all facioscapulohumeral muscular dystrophy patients with an *Eco*RI fragment size ranging from 10 to 25 kb, and each patient had a specific polymerase chain reaction product which corresponded to the size calculated from the number of D4Z4. Using southern blot analysis, more than 90% of facioscapulohumeral muscular dystrophy patients have a smaller *Eco*RI fragment than 26 kb in our series, and the number of D4Z4 repeats is precisely counted by this polymerase chain reaction method. We conclude that this long polymerase chain reaction method can be used as an accurate genetic screening technique for facioscapulohumeral muscular dystrophy patients.

Keywords: Facioscapulohumeral muscular dystrophy; Chromosome 4q35; Genetic diagnosis; Southern blotting; PCR; *Eco*RI fragment; D4Z4

1. Introduction

Facioscapulohumeral muscular dystrophy (FSHD) is a common autosomal dominant muscular disorder characterized by its distinct clinical presentation. It often involves weakness and atrophy of facial muscles, followed by shoulder-girdle, the scapula fixators, and the upper arm muscles. Subsequently, pelvic girdle and lower limbs are also affected. About 20% of the patients eventually become wheelchair-bound by 40 years of age [1]. Difficulties of whistling, eye closure, or arm raising are common initial symptoms. Prominent scapular winging and horizontally positioned clavicles are also observed. Facial or shoulder girdle weakness usually appears during adolescence, but signs may be apparent on examination even in early childhood. Asymmetry of muscle involvement is often observed in apparently affected patients, but this is unrelated to handedness [2]. Weakness is relatively mild and the progression is usually slow with frequent association of subclinical hearing loss and retinal vasculopathy. The clinical diagnosis of FSHD is sometimes difficult because the onset of illness and the phenotypic expression is extremely variable, both within and between families [3,4].

The gene locus for FSHD has been identified on chromosome 4q35 wherein an array of tandem repeat units is located. Each repeat is a 3.3-kb *Kpn*I digestable fragment designated as D4Z4 (Fig. 1) [5–7]. The disease is usually associated with a deletion of this repeated region, however the responsible gene has not yet been identified, and the underlying molecular mechanism is still enigmatic. Southern blot analysis using the probe p13E-11 (D4F104S1) [6] is usually performed in the genetic diagnosis of FSHD. Normal individuals have *Eco*RI digested fragments containing D4Z4 repeats which varies from 40 kb to more than 300 kb in size, however, most of the FSHD patients have a smaller sized fragment from 10 to 35 kb. The clinical severity is often correlated to the fragment size, and patients with the smallest *Eco*RI fragment show very early onset and can be associated with epilepsy and mental retardation [8,9].

* Corresponding author. Tel.: +81 42 341 2712; fax: +81 42 346 1742.
E-mail address: hayasi_y@ncnp.go.jp (Y.K. Hayashi).

0960-8966/$ - see front matter © 2006 Elsevier B.V. All rights reserved.
doi:10.1016/j.nmd.2006.01.008

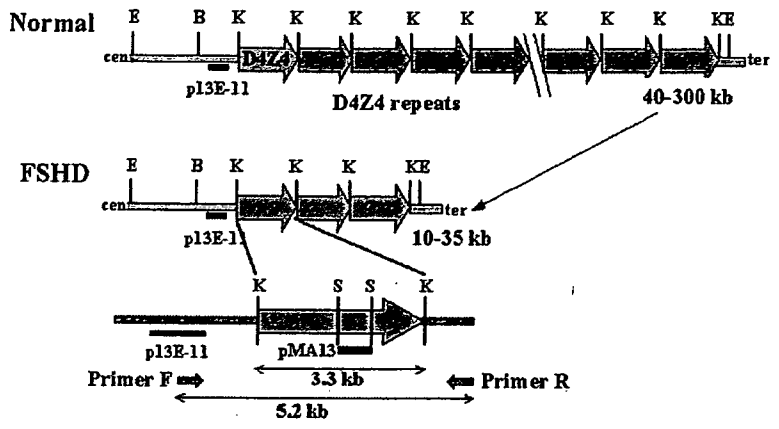

Fig. 1. A schematic diagram of the FSHD gene region on chromosome 4q35 showing the relative locations of primers and the probes used in this study. The primer set has been designed in the non-repeated region, and is expected to produce a 5.2 kb PCR amplified product when template genomic DNA contains one D4Z4 repeat. Cen, centromeric side of the gene; ter, telomeric side of gene; E, *Eco*RI; B, *Bln*I; K, *Kpn*I; S, *Sal*I.

Presently, the accuracy of the molecular diagnosis for FHSD using southern blot is up to 98% [10], however, several factors make this method cumbersome, and more than a week-length of time is required to obtain the results. In the conventional southern blotting method, it is difficult to resolve fragment size over 50 kb, and pulsed-field gel electrophoresis (PFGE) is sometimes taken together to increase resolution. Somatic and germline mosaicism is frequently observed in which more than three different sized *Eco*RI fragments on chromosome 4q are identified [11,12]. Furthermore, homologous 3.3-kb repeat-like sequences are also identified on many other chromosomes such as chromosomes Y and 3p [13,14]. In addition, chromosome 10q26 also contains 3.3-kb *Kpn*I digestable tandem repeats with 98% nucleotide identity to D4Z4 on chromosome 4 [15,16]. Consequently, there is a high incidence of inter-chromosomal exchange between 4q35 and 10q26, which is observed in about 20% of normal individuals [17,18]. In southern blot analysis, the probe p13E-11 used is not specific only to recognize *Eco*RI fragment from chromosome 4q but can also identify *Eco*RI fragment on chromosomes 10q26 and Y. This would require double restriction enzyme digestion using *Eco*RI and *Bln*I to be performed to distinguish 4q35-derived D4Z4 (*Bln*I-resistant) from 10q26-derived repeated units (*Bln*I-sensitive) [19]. From these complexities, there is an urgent need to develop a more simplified and reliable method for the diagnosis of FSHD.

Here, we introduce a new method to count the numbers of D4Z4 repeats on chromosome 4q35 by using long PCR amplification, which is quite useful for the rapid and accurate genetic diagnosis of FSHD.

2. Materials and methods

All clinical materials used in this study were acquired with informed consent. One hundred and five patients with a 4q-linked small *Eco*RI fragment from 10 to 35 kb (Table 3), and seven healthy individuals were examined. Genomic DNA was carefully and gently extracted from blood lymphocytes using a standard method. Southern blot analysis using the probe p13E-11 was performed as previously described [12].

For a long PCR amplification, a 50 μl reaction mixture was used. This mixture contains 400–600 ng of genomic DNA, 25 μl of 2× GC Buffer I (TAKARA BIO INC. Japan), 7.5 μl dATP/dTTP/dCTP mixture (10 mM each), 2.5 μl dGTP/7-deaza-dGTP mix (2:3), 1 μl (10 pM/μl) of each primers, and 0.5 μl (5 U/μl) LA Taq HS (TAKARA BIO). The primers were designed based on the human genomic sequences from GenBank (Accession Numbers D38025 and U74497). The primer sequences are F: 3′-GGCCAGAGTTT-GAATATACTGTGGTCATCTCTGCTCCAG-5′, R: 3′-CAGGGGATATTGTGACATATCTCTGCACTCATC. Amplification was performed using GeneAmp PCR System 9700 (PerkinElmer Japan Co., Ltd, Japan) with the following conditions; 1 min at 94 °C for the initial denaturation, followed by 10 cycles of 10 s at 98 °C and 20 min at 64 °C, and an additional 23 cycles of 10 s at 98 °C, 20 min with autoextension of 20 s per cycle at 64 °C, and 10 min at 72 °C for final elongation. The PCR products were separated by electrophoresis using 0.4% SeaKem HGT agarose gel (FMC BioProducts, ME) in 1× TAE with 0.5 μg/ml ethidium bromide at 3 h. High Molecular Weight DNA Marker (8.3–48.5 kb) (Invitrogen Japan K.K., Japan) and 1 kb plus ladder (Invitrogen) were used. The number of the 3.3 kb *Kpn*I repeated units in the FSHD gene region was calculated by the sequence data from GenBank (Accession Numbers D38024, D38025, and U74497).

In order to ascertain the specificity of the amplified products, we transferred the gels to Hybond N^+ (Amersham Biosciences, Japan) and overnight hybridization at 65 °C was performed with the ^{32}P-labeled probes of p13E-11 and pMA13 (1.3 kb *Stu*I fragment within a D4Z4 unit). The membrane was washed in a stringency of 2× SSC/0.1% SDS for 20 min at 65 °C for two times, followed by

Table 1
Comparison of long PCR and southern blot (SB) analyses

	PCR	SB
Template DNA (μg)	0.4	40
Enzyme digestion	No	*Eco*RI, *Bln*I
Gel size, concentration	11×14 cm, 0.4%	20×20 cm, 0.3%
Required time (h)		
PCR	11	0
Electrophoresis	3	68
Transfer	0	18
Hybridization	0	18
Detection	EB	RI
Total time required	<1 day	7–10 days
Accuracy (%)	90.1[a]	98 [10]

EB, ethidium bromide; RI, radio isotope.
[a] Estimated from the distribution of *Eco*RI fragment size in our series as described in Table 2.

autoradiography for 2 h using BAS2500 image analyzer (Fiji Photo Film, Japan).

3. Results

Table 1 shows the comparison of our newly developed long PCR method and the conventional southern blot analysis. This long PCR method is quite simple, requiring only a small amount of genomic DNA (1/100 of the quantity for southern blotting) and results are rapidly acquired overnight.

The long PCR method amplified five different sized products of 5.2, 8.5, 11.8, 15.1 and 18.4 kb which corresponded to the calculated size from the sequence data of the FSHD region containing one to five D4Z4 repeats, respectively (Fig. 2a, Table 3). These PCR products were not digested by *Bln*I, and were exclusively hybridized by the two probes of p13E-11 and pMA13 (data not shown). The same PCR method was performed on 10 individuals with a small *Eco*RI fragment (from 10 to 25 kb) on chromosome 10q26 but no amplified product was identified (data not shown).

Table 2 shows the distribution of the size of small *Eco*RI fragment on chromosome 4q of 263 FSHD families in our series. Table 3 shows the size of the PCR products, the calculated size of the *Eco*RI fragment, the range of the fragment size detected by southern blot analysis, and number of the patients. A 5.2 kb PCR product that contains one D4Z4 repeat was observed in eight patients with a *Eco*RI fragment from 10 to 11 kb. Sequence analysis confirmed that this 5.2 kb fragment contains one D4Z4 repeat on chromosome 4q35. An 8.5 kb band corresponding to the size with two D4Z4 repeated units was detected in 23 patients with 13–17 kb *Eco*RI fragment. An 11.8 kb product (three D4Z4 repeats) was seen in 26 patients with 16–19 kb fragment, a 15.1 kb fragment (four D4Z4 repeats) was seen in 24 patients with 18–22 kb fragment, and a 18.4 kb product (five D4Z4 repeats) was observed in six patients with 23–25 kb *Eco*RI fragment. The PCR products were amplified from all 87 DNA samples of the patients with an *Eco*RI fragment of 25 kb or less. However, DNA from normal individuals and FSHD patients with larger (≧26 kb) *Eco*RI fragments were not successfully amplified/detected by this long PCR method.

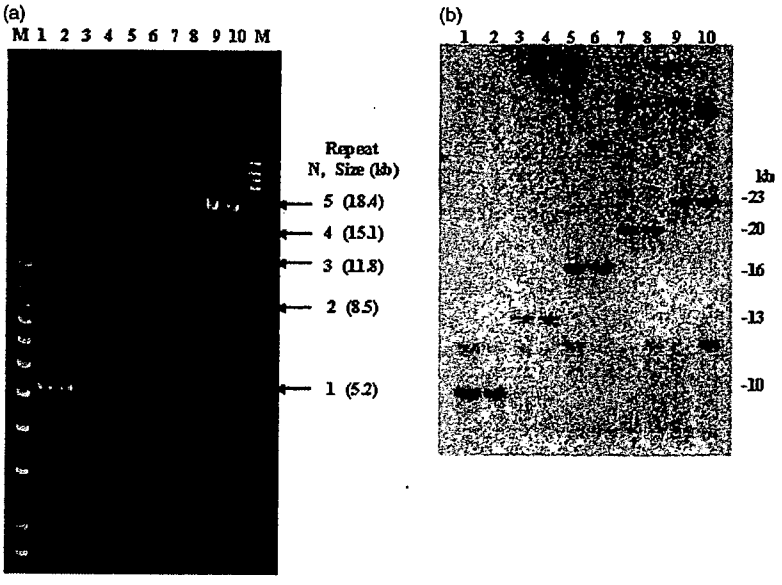

Fig. 2. Long PCR amplification and conventional southern blot analysis using genomic DNA from FHSD patients. (a) A 5.2 kb PCR product was detected on two patients with an *Eco*RI fragment of 10-kb (lane 1), or 11-kb (lane 2) as interpreted from our previous southern blot study. An 8.5-kb band was detected from two patients with a 13-kb (lane 3) or a 14-kb (lane 4) fragment, an 11.8-kb product from two patients with a 16-kb (lane 6) or a 17-kb (lane 7) fragment, a 15.1-kb product from a 20 or a 22 kb fragment, and an 18.4 kb fragment was identified from patients with a 24 and a 25 kb *Eco*RI fragment. These PCR products correspond to the size containing one to five D4Z4 repeated units. (b) Southern blot analysis using the same 10 samples in (a). The samples with the same size of the PCR products showed no difference of the *Eco*RI fragment size, although variable fragment size was previously interpreted.

Table 2
Distribution of *Eco*RI fragment size on chromosome 4q of 263 families in our series

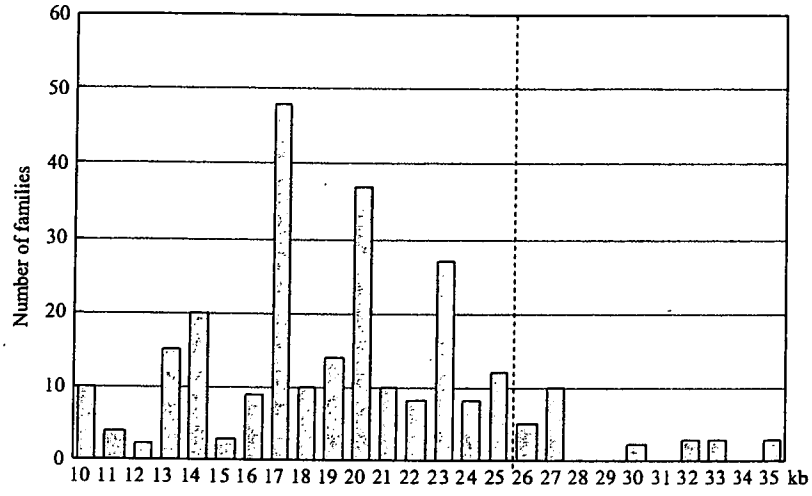

*Eco*RI fragments of <26 kb (dot line) can be amplified by long PCR analysis.

Estimated fragment size from the previous southern blot was not identical among the patients with same numbers of D4Z4 repeats. To determine the inter-individual variability of the fragment size, conventional southern blot analysis was repeated simultaneously. Notably, after the repeated southern blot technique, the *Eco*RI fragment size was similar when the D4Z4 number was the same and this result was consistent with the calculated size (Fig. 2b).

4. Discussions

In this study, we have successfully developed a new method for rapid and specific diagnosis of FSHD by counting the number of D4Z4 repeats via a long PCR amplification technique. This long PCR method can specifically amplify the repeated region from chromosome 4q up to 18.4 kb in size and countable from one to five D4Z4 repeated units.

Table 3
Comparison of the results of long PCR and southern blot (SB) analysis

Number of D4Z4 repeats	PCR product size (kb)	Calculated size of *Eco*RI fragment (kb)	Range of *Eco*RI fragment by SB (kb)	Number of patients examined by PCR
1	5.2	10.2	10-11	8
2	8.5	13.5	13–17	23
3	11.8	16.8	16–19	26
4	15.1	20.1	18–22	24
5	18.4	23.4	23–25	6
6	21.7	26.7	26–35	18
7	25	30		
8	28.3	33.3		(No amplification)
9	31.6	36.6		

D4Z4 repeat has highly GC-rich sequence up to 73% [20]. Difficulties in PCR amplification often arise when GC content of the template DNA exceeds 50%. This difficulty in PCR amplification was overcame in our study by using thermo-stable long accurate Taq, 7-deaza-dGTP, and a higher denaturing temperature (98 °C) followed by a relatively higher annealing/extension temperature (64 °C) for 20 min with autoextension of 20 s per cycle. Therefore 73% of GC-containing repeated region of more than 18 kb in size was amplified with ease. The specificity of each PCR amplified product was ascertained by several ways. First, both probes (p13E-11 and pMA-13) that were used in the hybridization of the PCR products exclusively recognize fragments containing D4Z4 repeats. Second, the restriction enzyme *Bln*I did not digest the amplified fragments and confirmed that the product is apparently different from the repeats derived from chromosome 10q26, wherein 98% homologous *Kpn*I repeated units and franking sequences are known. Third, this long PCR method did not amplify *Kpn*I repeats from 10q26 even though the only difference is one different nucleotide from each of the primer region on 4q35. We also designed 10q-specific primer set and confirmed that only the 10q-derived repeats could be amplified by using this primer set.

The diagnosis of FSHD is sometimes difficult. Clinical symptoms and severity are quite variable between the patients even within the same family. Up to date, genetic diagnosis of FSHD is solely depended on the southern blot analysis since no responsible gene is yet identified within the candidate region. However, such procedure requires a large amount of DNA and would necessitate at least a week-time period to produce results. The requirement for such

amount of time for analysis dwells on the complexity of the experimental protocols in detecting the various fragments, the sizes ranging from 10 to 300 kb, as well as the determination of the existence of homologous regions on the other chromosomes. Determination of the size of *Eco*RI fragment is important since it is usually correlated to the clinical severity. However, identification of the precise fragment size is often difficult in the conventional southern blotting, since only very low concentrated gels of 0.3% is used to detect large sized fragment, and even minor changes in the experimental conditions would produce different results. In fact, in our very own series, DNA samples containing the same number of D4Z4 repeats showed the same *Eco*RI fragment size on one membrane although the estimated size in our previous analysis detected by different membranes were variable. Therefore, the number of D4Z4 units estimated from the *Eco*RI fragment size using Southern blotting could be misinterpreted from its actual number. From the result of the long PCR analysis, we concluded that the number of D4Z4 is countable from the size of PCR products, and the deletion of the FSHD region is certainly caused by the deleted integral number of D4Z4.

The number of D4Z4 is specifically countable up to five, which corresponds to the estimated *Eco*RI fragment of 10–25 kb in size. When no amplified product was obtained, southern blot analysis is required. In our series, 9.9% of the 4q-linked small *Eco*RI fragments have 26–35 kb as shown in Table 2, but the percentage may be greater in other countries. In the cases having deletion of p13E-11, no product can be obtained in this PCR analysis, since the forward primer is designed within this region. However, considering the complexity of the southern blot technique, this long PCR analysis is useful for the initial screening of the FSHD patients, and also the genetic test for the other family members with a known D4Z4 repeat numbers from 1 to 5 in an index patient. Obtaining accurate results rapidly is always beneficial for the patient, especially during prenatal test. From the economical point of view, PCR analysis is also beneficial since it costs 1/30–40 for the southern blot analysis.

Both primer sequences we used in this study are 4q-specific, and can amplify fragments even those with zero D4Z4 repeat, if any, producing an estimated 1.9-kb product. We also designed a primer set that can specifically amplify the repeated region on chromosome 10q. Theoretically, by using several combinations of these primers, we should be able to distinguish rare cases with short hybrid repeats on 4q or non-FSHD *Bln*I-resistant fragments on 10q. We concluded that the long PCR method could be used as an accurate genetic screening technique for FSHD.

Acknowledgements

We would like to thank Dr Mina Nolasco Astejada (NCNP) for critically reviewing the manuscript. This work was supported by Health and Labor Science Research Grants, Research on Psychiatric and Neurological Diseases and Mental Health, and The Research Grant (17A-10) for Nervous and Mental Disorders from the Ministry of Health, Labour and Welfare, Research on Health Sciences focusing on Drug Innovation from The Japan Health Sciences Foundation, Japan.

References

[1] Lunt PW, Harper PS. Genetic counselling in facioscapulohumeral muscular dystrophy. J Med Genet 1991;28:655–64.
[2] Tawil R, McDermott MP, Mendell JR, Kissel J, Griggs RC. Facioscapulohumeral muscular dystrophy (FSHD): design of natural history study and results of baseline testing, FSH-DY group. Neurology 1994;44:442–6.
[3] Lunt PW, Jardine PE, Koch M, et al. Phenotypic–genotypic correlation will assist genetic counseling in 4q35-facioscapulohumeral muscular dystrophy. Muscle Nerve 1995;2:S103–S9.
[4] Padberg GW, Frants RR, Brouwer OF, Wijmenga C, Bakker E, Sandkuijl LA. Facioscapulohumeral muscular dystrophy in the Dutch population. Muscle Nerve 1995;2:S81–S4.
[5] Upadhyaya M, Lunt P, Sarfarazi M, Broadhead W, Farnham J, Harper PS. The mapping of chromosome 4q markers in relation to facioscapulohumeral muscular dystrophy (FSHD). Am J Hum Genet 1992;51:404–10.
[6] Wijmenga C, Hewitt JE, Sandkuijl LA, et al. Chromosome 4q DNA rearrangements associated with facioscapulohumeral muscular dystrophy. Nat Genet 1992;2:26–30.
[7] Hewitt JE, Lyle R, Clark LN, et al. Analysis of the tandem repeat locus D4Z4 associated with facioscapulohumeral muscular dystrophy. Hum Mol Genet 1994;3:1287–95.
[8] Funakoshi M, Goto K, Arahata K. Epilepsy and mental retardation in a subset of early onset 4q35-facioscapulohumeral muscular dystrophy. Neurology 1998;50:1791–4.
[9] Miura K, Kumagai T, Matsumoto A, et al. Two cases of chromosome 4q35-linked early onset facioscapulohumeral muscular dystrophy with mental retardation and epilepsy. Neuropediatrics 1998;29: 239–41.
[10] Upadhyaya M, Cooper DN. Molecular diagnosis of facioscapulohumeral muscular dystrophy. Expert Rev Mol Diagn 2002;2: 160–71.
[11] Lemmers RJ, van der Wielen MJ, Bakker E, Padberg GW, Frants RR, van der Maarel SM. Somatic mosaicism in FSHD often goes undetected. Ann Neurol 2004;55:845–50.
[12] Goto K, Nishino I, Hayashi YK. Very low penetrance in 85 Japanese families with facioscapulohumeral muscular dystrophy 1A. J Med Genet 2004;41:e12.
[13] Clark LN, Koehler U, Ward DC, Wienberg J, Hewitt JE. Analysis of the organisation and localisation of the FSHD-associated tandem array in primates: implications for the origin and evolution of the 3.3 kb repeat family. Chromosoma 1996; 105:180–9.
[14] Ballarati L, Piccini I, Carbone L, et al. Human genome dispersal and evolution of 4q35 duplications and interspersed LSau repeats. Gene 2002;296:21–7.
[15] Deidda G, Cacurri S, Grisanti P, Vigneti E, Piazzo N, Felicetti L. Physical mapping evidence for a duplicated region on chromosome 10qter showing high homology with the facioscapulohumeral muscular dystrophy locus on chromosome 4qter. Eur J Hum Genet 1995;3:155–67.

[16] van Geel M, Dickson MC, Beck AF, et al. Genomic analysis of human chromosome 10q and 4q telomeres suggests a common origin. Genomics 2002;79:210–7.
[17] Matsumura T, Goto K, Yamanaka G, et al. Chromosome 4q;10q translocations; comparison with different ethnic populations and FSHD patients. BMC Neurol 2002;2:7.
[18] Lemmers RJ, van der Maarel SM, van Deutekom JC, et al. Inter- and intrachromosomal sub-telomeric rearrangements on 4q35: implications for facioscapulohumeral muscular dystrophy (FSHD) aetiology and diagnosis. Hum Mol Genet 1998;7: 1207–14.
[19] Deidda G, Cacurri S, Piazzo N, Felicetti L. Direct detection of 4q35 rearrangements implicated in facioscapulohumeral muscular dystrophy (FSHD). J Med Genet 1996;33:361–5.
[20] Lee JH, Goto K, Matsuda C, Arahata K. Characterization of a tandemly repeated 3.3-kb KpnI unit in the facioscapulohumeral muscular dystrophy (FSHD) gene region on chromosome 4q35. Muscle Nerve 1995;2:S6–S13.

Human Molecular Genetics, 2006, Vol. 15, No. 8 1279–1289
doi:10.1093/hmg/ddl045
Advance Access published on March 10, 2006

Aberrant neuromuscular junctions and delayed terminal muscle fiber maturation in α-dystroglycanopathies

Mariko Taniguchi[1], Hiroki Kurahashi[3], Satoru Noguchi[4], Takayasu Fukudome[5], Takeshi Okinaga[2], Toshifumi Tsukahara[6], Youichi Tajima[7], Kelichi Ozono[2], Ichizo Nishino[4], Ikuya Nonaka[4] and Tatsushi Toda[1,*]

[1]Division of Clinical Genetics, Department of Medical Genetics and [2]Department of Pediatrics, Osaka University Graduate School of Medicine, 2-2 Yamadaoka, Suita, Osaka 565-0871, Japan, [3]Division of Molecular Genetics, Institute for Comprehensive Medical Science, Fujita Health University, Toyoake, Aichi 470-1192, Japan, [4]National Institute of Neuroscience, National Center of Neurology and Psychiatry, Kodaira, Tokyo 187-8502, Japan, [5]Division of Clinical Research, Nagasaki Medical Center of Neurology, Kawatanamachi, Nagasaki 859-3615, Japan, [6]Center for Nano Materials and Technology, Japan Advanced Institute of Science and Technology, Tatsunokuchi, Ishikawa 923-1292, Japan and [7]Department of Clinical Genetics, The Tokyo Metropolitan Institute of Medical Science, Bunkyo-ku, Tokyo 113-8613, Japan

Received October 15, 2005; Revised and Accepted February 28, 2006

Recent studies have revealed an association between post-translational modification of α-dystroglycan (α-DG) and certain congenital muscular dystrophies known as secondary α-dystroglycanopathies (α-DGpathies). Fukuyama-type congenital muscular dystrophy (FCMD) is classified as a secondary α-DGpathy because the responsible gene, *fukutin*, is a putative glycosyltransferase for α-DG. To investigate the pathophysiology of secondary α-DGpathies, we profiled gene expression in skeletal muscle from FCMD patients. cDNA microarray analysis and quantitative real-time polymerase chain reaction showed that expression of developmentally regulated genes, including myosin heavy chain (*MYH*) and myogenic transcription factors (*MRF4*, *myogenin* and *MyoD*), in FCMD muscle fibers is inconsistent with dystrophy and active muscle regeneration, instead more of implicating maturational arrest. FCMD skeletal muscle contained mainly immature type 2C fibers positive for immature-type MYH. These characteristics are distinct from Duchenne muscular dystrophy, suggesting that another mechanism in addition to dystrophy accounts for the FCMD skeletal muscle lesion. Immunohistochemical analysis revealed morphologically aberrant neuromuscular junctions (NMJs) lacking MRF4 co-localization. Hypoglycosylated α-DG indicated a lack of aggregation, and acetylcholine receptor (AChR) clustering was compromised in FCMD and the myodystrophy mouse, another model of secondary α-DGpathy. Electron microscopy showed aberrant NMJs and neural terminals, as well as myotubes with maturational defects. Functional analysis of NMJs of α-DGpathy showed decreased miniature endplate potential and higher sensitivities to *d*-Tubocurarine, suggesting aberrant or collapsed formation of NMJs. Because α-DG aggregation and subsequent clustering of AChR are crucial for NMJ formation, hypoglycosylation of α-DG results in aberrant NMJ formation and delayed muscle terminal maturation in secondary α-DGpathies. Although severe necrotic degeneration or wasting of skeletal muscle fibers is the main cause of congenital muscular dystrophies, maturational delay of muscle fibers also underlies the etiology of secondary α-DGpathies.

*To whom correspondence should be addressed. Tel: +81 668793380; Fax: +81 668793389; Email: toda@clgene.med.osaka-u.ac.jp

INTRODUCTION

Fukuyama-type congenital muscular dystrophy (FCMD; MIM 253800) is an autosomal recessive muscular dystrophy and the second most common childhood muscular dystrophy in Japan, following Duchenne muscular dystrophy (DMD) (1). Clinical manifestations of FCMD include severe congenital muscular dystrophy from early infancy, cobblestone lissencephaly and eye malformation. We previously isolated the responsible gene for FCMD, termed *fukutin* (2,3). Recently, it has been postulated that *fukutin* modulates the glycosylation of α-dystroglycan (α-DG), a major component of the dystrophin–glycoprotein complex (4,5). FCMD is classified as one of the congenital muscular dystrophies, such as laminin-α2-deficient congenital muscular dystrophy (MDC1A) (6). Recently, FCMD has also been classified as a secondary α-DGpathy, as mutations in genes encoding glycosyltransferases result in hypoglycosylated α-DG (7). α-Dystroglycan binds to extracellular matrix proteins such as laminin, agrin and perlecan, which are important in maintaining muscle cell integrity (8). Hypoglycosylated α-DG provokes the post-translational disruption of dystroglycan–ligand interactions in the skeletal muscle of patients, leading to the severe phenotypes of congenital muscular dystrophies (7). Other glycosyltransferases include POMGnT1 (protein *O*-mannose β-1, 2-*N*-acetylglucosaminyltransferase 1), POMT1 and POMT2 (protein *O*-mannosyltransferases 1 and 2), fukutin-related protein (FKRP) and LARGE; mutations in these genes induce human muscle–eye–brain disease, Walker–Warburg syndrome and congenital muscular dystrophy type 1C/1D, and mouse myodystrophy, respectively (9–14).

Primary characteristics of the so-called 'muscular dystrophy' such as DMD include necrotic change and active regeneration of muscle fibers. From infancy, DMD patients usually show dystrophic change in skeletal muscle, accompanied by elevation of serum creatine kinase (CK) levels. However, DMD patients usually maintain their gait until early adolescence. In contrast, FCMD patients show severe phenotypic characteristics from very early infancy, and few patients can acquire gait regardless of serum CK levels (1). Skeletal muscle fibers in FCMD are extremely small, irregular in cell size and architecturally disorganized, and extensive fibrosis prevails from the early infantile stage. However, only a small number of muscle fibers show severe necrotic change or active myofibril regeneration, and satellite cells are also fewer than those of DMD (1,15,16). These phenotypic differences promote the hypothesis that another mechanism may also account for the pathophysiology of secondary α-DGpathies.

Although expression profiling of skeletal muscle from patients with DMD, MDC1A and α-sarcoglycanopathy have been described (17–19), no similar analysis has been reported for FCMD and other secondary α-DGpathies. To investigate the molecular mechanism of FCMD and other secondary α-DGpathies, we profiled gene expression in FCMD skeletal muscle using cDNA microarray and subsequent quantitative real-time polymerase chain reaction (PCR). Here we demonstrate that aberrant neuromuscular junctions (NMJs) and maturational delay of muscle fibers are significant to the mechanism underlying secondary α-DGpathies.

RESULTS

Aberrant muscle regeneration is suggested by gene expression profiling of FCMD skeletal muscle

Gene expression profiling of FCMD skeletal muscle was performed using a custom cDNA microarray. Clustering analysis showed similar overall expression profiles of muscle from four FCMD patients, aged 20 days to 1 year, 6 months (Fig. 1A). This similarity is independent of age and histology of the muscle specimen in our samples.

We analyzed individual genes showing distinct expression patterns in FCMD skeletal muscle compared with normal children or DMD patients. Most genes encoding muscle components were down-regulated in FCMD. Among these, *myosin light chain 1, 3* and *4* (*myl1, 3* and *4*) were up-regulated in DMD skeletal muscle, in contrast with FCMD (Fig. 1B). Expression of the developmentally regulated myosin heavy chains (*MYHs*), *MYH1*, *MYH2* and *MYH7* (slow, adult-type), was down-regulated in FCMD but not in DMD, whereas expression of *MYH8* (fast-type) showed no significant change in FCMD compared with DMD or normal controls. Slow-type MYHs (MYH1, MYH2 and MYH7) are present in mature muscle fibers and crucial for sarcomere assembly to maintain muscle integrity, whereas fast-type or developmental MYHs (MYH3, MYH4 and MYH8) are seen in early immature myoblasts or in regenerating fibers. These observations suggest that expression of mature muscle components is suppressed in FCMD skeletal muscle at all ages examined.

With regard to muscle fiber differentiation, myogenic factors including *MyoD*, *myf5* and *myogenin* (*myf4*) showed insufficient signal for the analysis. It is noteworthy, however, that *MRF4* (*myf6*) was down-regulated in FCMD. Expression of the alpha-type cholinergic receptor (*CHRNA*), which is known to be regulated by *MyoD* and *MRF4* (20,21), was much higher in FCMD patients than in normal controls.

We next performed real-time quantitative PCR to further investigate skeletal muscle differentiation. We compared mRNA expression in FCMD muscle with normal or DMD skeletal muscle, as DMD is a good example for active regeneration, in which expression of muscle component and myogenic factor mRNA expression is expected to be up-regulated. Although *CHNRA* was up-regulated in DMD, as predicted, its expression was even higher in FCMD (Fig. 2A and B). Among these cholinergic receptor subtypes, gamma-type cholinergic receptor (*CHNRG*), which is a component of fetal isoforms, was up-regulated, whereas epsilon-type cholinergic receptor (*CHNRE*), which only composes adult isoforms (22), was down-regulated in FCMD (Fig. 2B). MYH slow-type (*MYH7*) was down-regulated in FCMD, consistent with the microarray analysis, whereas expression of fast-type MYH (*MYH11b*) was not altered in FCMD. Interestingly, although *MyoD* and *myogenin* were up-regulated in both DMD and FCMD, *MRF4* was down-regulated in FCMD muscle but up-regulated in DMD (Fig. 2A and B). *MRF4* expression is known to be up-regulated in the late phase of muscle regeneration or differentiation, followed by sequential expression of *MyoD*, *myf5* and *myogenin*, indicating significant roles in terminal differentiation (20,21). These results suggest that FCMD skeletal muscle undergoes an unbalanced differentiation process.

A

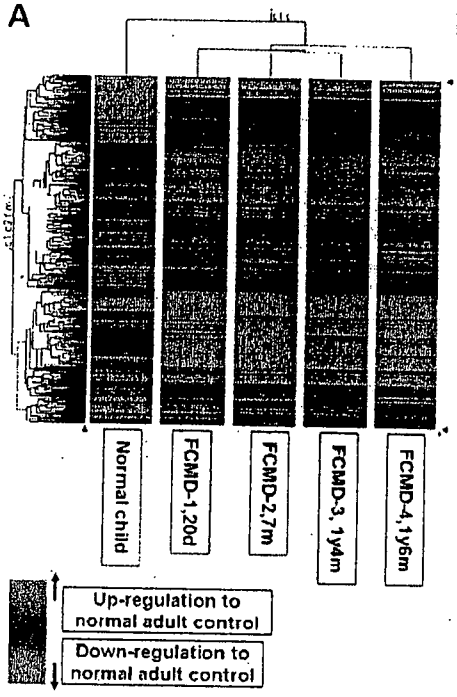

B

gene	FCMD	DMD	Product
myl1	↓	→	myosin light chain 1
myl2	↓	↑	myosin light chain 2
myl3	↓	↑	myosin light chain 3
myl4	↓	↑	atrial /embryonic alkali myosin light chain
myh1	↓↓	↑	myosin, heavy polypeptide 1, adult (slow)
myh2	↓↓	↑	myosin, heavy polypeptide 2, adult (slow)
myh7	↓↓	↑	myosin, heavy polypeptide 7, beta (slow)
myh8	↓	→	myosin, heavy polypeptide 8, (fast)
myhbpc1	↓↓	↑	myosin binding protein C, slow type
myhbph	↑	→	myosin-binding protein H
actc	↑	↑	actin, alpha, cardiac muscle precursor
actg1	↓	↑	actin, gamma 1
actg2	↓	↑↑	actin, gamma 2
sgcb	↓↓	↓	sarcoglycan, beta
tcap	↓↓	→	titin-cap (telethonin)
ttn	↓↓	↓	titin
des	↓↓	↑	desmin
myf6	↓	→	MRF4 (myf6,herculin)
CHRNA	↑↑	→	nicotinic type, acetylcholine receptor

Figure 1. Cluster image and gene trees from expression profiling of FCMD and normal skeletal muscle. (A) Each line corresponds to the expression signal of each gene. Genes are ordered using the average linkage clustering method to group similar expression profiles. Red denotes up-regulated genes and green denotes down-regulated genes compared with adult control muscle. Note that the expression trends are almost identical within FCMD patients, and FCMD trends are distinct from those of normal children. (B) Expression profile of major muscle components of FCMD and DMD compared with that of normal children. Arrows show the relative expression change (single upward arrow and downward arrow, more than 2-fold increase/decrease; double upward arrows and downward arrows, more than 10-fold increase/decrease; rightward arrow, no change). Note that majority of muscle components are down-regulated in FCMD muscles.

Final maturation step is retarded in FCMD skeletal muscle

To investigate how differentiation is impaired, we examined histological specimens of FCMD skeletal muscle. Marked interstitial tissues with numerous small, round-shaped immature fibers and some necrotic fibers increased with age were seen in FCMD skeletal muscle specimens. Interstitial tissue is prominent from early infancy and progresses with age (Fig. 3A–C), and skeletal muscle from an FCMD fetus also shows rich interstitial tissues (Fig. 3E). Although necrotic change in muscle fibers is not so marked as in DMD fibers, DMD muscle shows less marked fibrosis and more mature fibers, despite more active necrotic and regenerating processes (Fig. 3D). Overall, FCMD muscle is reminiscent of fetal muscle; skeletal muscle from a normal fetus appears rich in fibrous tissues and small, round-shaped immature myotubes (Fig. 3F).

Muscle fiber type is easily identified by ATPase staining. Normally, type 2C fibers are mainly seen in fetal muscle fibers or in regenerating fibers. However, in ATPase-stained cryospecimens, FCMD muscle showed a significantly higher percentage of undifferentiated type 2C muscle fiber contents relative to DMD or control samples ($P < 0.005$) (Fig. 3G and H, Table 1).

Using immunohistochemical analysis, we examined MYH subtypes to confirm the differentiation impairment in FCMD and in myodystrophy mouse (*myd*), which is another model of secondary α-DGpathies. In normal muscle from age-matched controls, no staining of developmental or neonatal MYH (Fig. 3I and J) was seen. In contrast, FCMD and *myd* muscle fibers stained positively for developmental and neonatal MYHs (Fig. 3M and N). These positive fibers corresponded with those staining positive for fast-type MYHs in a serial section (Fig. 3M–O, arrows). Similar staining patterns were observed in skeletal muscle from an FCMD fetus. It is unlikely that all fibers showing developmental MYH expression are derived from regenerating fibers, as few active regenerating or necrotic fibers are seen in the hematoxylin and eosin (HE) specimen at any ages (Fig. 3A–C). Similar staining patterns were observed in skeletal muscles from an FCMD fetus and adult *myd* (data not shown). It is unlikely that all fibers showing developmental MYH expression are derived from regenerating fibers, as few active regenerating or necrotic fibers are seen in the HE specimen (Fig. 3A–C).

These results induce the possibility that maturation might be slowed or arrested in FCMD and *myd* skeletal muscles, and possibly this is common in secondary α-DGpathies. It also